Terminal Synergetic Control with the Dragonfly Algorithm for Zoonotic Visceral Leishmaniasis Eradication

Tinnakorn Kumsaen
Department of Chemical Engineering, Faculty of Engineering, Khon Kaen University, Thailand
tinnakor@kku.ac.th

Arsit Boonyaprapasorn
Department of Mechanical Engineering, Chulachomklao Royal Military Academy, Nakhon-Nayok, Thailand
arsit.bo@crma.ac.th

Settapat Chinviriyasit
Department of Mathematics, Faculty of Science, King Mongkut's University of Technology Thonburi, Bangkok, Thailand
settapat.chi@kmutt.ac.th

Parinya Sa-Ngiamsunthorn
Department of Mathematics, Faculty of Science, King Mongkut's University of Technology Thonburi, Bangkok, Thailand
parinya.san@kmutt.ac.th

Thunyaseth Sethaput
Department of Mechanical Engineering, Sirindhorn International Institute of Technology, Thammasat University, Pathum Thani, Thailand
thunyaseth@siit.tu.ac.th

Thavida Maneewarn
Institute of Field Robotics (FIBO), King Mongkut's University of Technology Thonburi, Bangkok, Thailand
praew@fibo.kmutt.ac.th

Eakkachai Pengwang
Institute of Field Robotics (FIBO), King Mongkut's University of Technology Thonburi, Bangkok, Thailand
eakkachai.pen@kmutt.ac.th. (corresponding author)

Received: 31 July 2024 | Revised: 4 October 2024 and 22 October 2024 | Accepted: 26 October 2024

 DOI: https://doi.org/10.48084/etasr.8561

ABSTRACT

Visceral Leishmaniasis (VL) is a prevalent vector-borne disease that affects both human and animal populations in subtropical and tropical regions, contributing to a substantial mortality rate. Establishing efficient control policies is crucial to eradicating the VL epidemic. The VL epidemic system, containing reservoirs, vectors, and human populations, can be accurately modeled through differential equations. Managing the VL epidemic under multiple control policies can be considered a high-order nonlinear feedback control challenge. This study explores the application of Terminal Synergetic Control (TSC) to

eradicate Zoonotic Visceral Leishmaniasis (ZVL). Notably, Synergetic Control (SC) is one of the suitable feedback control methods for manipulating high-order nonlinear systems, providing practical control inputs because of their chattering-free behavior. Additionally, the convergence properties of the control system can be enhanced through terminal attraction. Optimization of control parameters within the system is achieved through the integration of control mechanisms by the Dragonfly Algorithm (DA). The results demonstrate that the multiple control policies synthesized by the TSC method effectively regulate subpopulations in alignment with the specified control objectives. Furthermore, the enhanced convergence rate achieved by the TSC method, in comparison to the SC method, serves as evidence of TSC's effectiveness in guiding the dynamics of ZVL epidemic eradication. This research underscores the potential of the TSC method, utilizing optimal control parameters provided by the DA, to achieve targeted outcomes with improved convergence properties.

Keywords-terminal synergetic control; feedback control; dragonfly algorithm; swarm-based algorithm; metaheuristic algorithm; zoonotic visceral leishmaniasis; epidemic system; vaccination

I. INTRODUCTION

Leishmaniasis is an epidemic disease that has become a significant concern, especially for impoverished populations [1]. The disease is caused by Leishmania, an intracellular flagellated protozoan that belongs to the family Trypanosomatidae, order Kinetoplastida [2, 3]. Leishmaniasis is transmitted by the bite of the female phlebotomine sandfly. Depending on the host's immune response and the virulent factors of the parasite, leishmaniasis can cause different forms of clinical manifestations, including Cutaneous Leishmaniasis (CL), Mucocutaneous Leishmaniasis (MCL), and Visceral Leishmaniasis (VL). Among these symptoms, the most serious is the visceral infection known as kala-azar [1, 4]. According to the mode of transmission, visceral leishmaniasis is classified as Anthroponotic Visceral Leishmaniasis (AVL) and Zoonotic Visceral Leishmaniasis (ZVL) [5]. Both human and vertebrate animals, especially dogs, cats, and rodents, can serve as reservoir hosts for transmission [1, 4]. In terms of epidemiology, leishmaniasis is endemic in subtropical and tropical regions in 98 countries [1, 4, 6]. WHO records showed that up to 350 million people were at risk of leishmaniasis contraction [1], with 0.7-1 million incidents of such infection [7] and 20,000-30,000 casualties yearly [6]. At present, the development of a vaccine for humans is still in progress [8]. The effectiveness of eradication of the leishmaniasis spread depends on the control of the sandfly vector and any reservoir hosts along with early diagnosis and appropriate treatment [7].

Epidemic models of VL for both anthroponotic and zoonotic modes have been developed and represented in previous works [9-14]. The growth rates of different subpopulations and control policies were included in the models to describe the dynamic subpopulations of the leishmaniasis epidemic systems. These dynamic epidemic models include multiple groups of populations, such as reservoir, vector, and human populations. The growth rate of the subpopulations in one group of population is affected by other subpopulations in both the same and other groups. Each population group consists of various subpopulations, for example, susceptible, exposed, infected, recovered, hospitalized, etc. Thus, popular models and their modified versions, such as SI, SIR, SEIR, SEIHR, and others, were used to construct VL epidemic models [9-14]. Typically, the control policy can be obtained by formulating a dynamic optimization problem. Then, optimal control can be determined by Pontryagin's maximum principle [9-14].

As the dynamics of the ZVL epidemic systems can be represented in the form of various compartment models, it is feasible to set the control strategies or policies to control the epidemic disease by using the optimal control according to Pontryagin's maximum principle, as shown in [10, 13, 14]. However, finding the control for biological systems based on optimal control requires an accurate model, and it is complex to find the control policy in analytical form for a high-order system [15]. Feedback control can be applied to establish the epidemic control policy. Using feedback control for setting the policy can be performed under the effects of uncertainties and disturbances [15]. Moreover, formulating the control policy in analytical form using a feedback control approach is comparatively more straightforward compared to employing the optimal control approach [15]. Consequently, formulating the control policy for eradicating epidemic systems, as represented by the corresponding compartment model, becomes both effective and efficient [15].

Feedback control theory has been used successfully to formulate control policies for eradicating different epidemic diseases, such as SARs, Influenza, Ebola, Tuberculosis, Hepatitis-B, HIV, and COVID-19 [15-35]. In this approach, the procedure for designing feedback controllers from widely recognized nonlinear control techniques, such as sliding mode control, feedback linearization, and synergetic control, was employed to formulate the control policies [15-36]. Related knowledge is also utilized to achieve the desired characteristics or enhance the performance of the control system, such as control of an epidemic system with time delay, observer-based control, and robustness, which were also considered in this approach [23, 30, 31, 33, 34, 37, 38]. Synergetic Control (SC) theory, following the Analytical Direct Aggregation Regulator (ADAR) method, can be effectively employed for vector-borne epidemic systems. This is particularly applicable as these systems pose high-order control problems involving multiple inputs and multiple outputs. The SC method, formulated in [39-41], allows the designer, using an appropriate set of macro variables, to establish a control law ensuring global stability. This method is capable of addressing issues arising from noise and parameter sensitivity [42, 43]. In the design process of the SC method, the control inputs are solved simultaneously [39-46]. Previous works have presented various applications of the SC method, such as power systems [42, 43, 46], mechanical systems [47-49], biomedical systems [51], and epidemic systems [21, 22]. According to [36, 50-52], the Terminal Synergetic Control (TSC) scheme has the potential to improve

the convergence properties of the control system. However, designers face the challenge of the singularity problem that can arise in the control input signal [53]. To address this problem, the combination of the terminal attraction approach with the integral expression has been proven to be an effective solution [53, 54].

In this study, the optimal set of control parameters is determined using the swarming behavior of dragonflies. The Dragonfly Algorithm (DA) is a nature-inspired optimization technique, classified as a metaheuristic algorithm within the broader range of swarm intelligence algorithms, originally introduced in [55]. The algorithm mimics the collective behavior and communication strategies observed in dragonfly swarms, demonstrating its efficiency in exploring solution spaces and identifying optimal solutions for numerical problems. The versatility of DA extends to various applications, including control systems [56]. When applied to tuning control parameters, the DA automatically fine-tunes the parameter values in a control system, contributing to the optimization of its performance. In the field of statistical modeling, the DA serves as a powerful tool to fine-tune control model parameters, ensuring that the system performance is optimized based on real-world data. Since control systems often involve nonlinearity, noise, and uncertainty, DA provides an effective solution by offering a robust mechanism to identify optimal control policies. It also aligns with the broader trend in research towards using bio-inspired algorithms to address complex optimization problems across various fields, including control engineering and machine learning [57]. Based on the benefits of employing the TSC method and DA, the primary focus of this study is to determine control policies capable of eradicating the epidemic of the ZVL system. This is achieved by using the proposed TSC method coupled with the DA to adjust the control parameters. The integral expression is introduced to avoid the singularity issue in the control input. Simulations were employed to illustrate and validate the performance of these control policies. The improvement in convergence rate can be assessed by comparing the proposed TSC method with the conventional SC method. The highlights of this study are as follows:

- The TSC method has not been used to establish a policy with multiple measures for the ZVL epidemic system. Implementing the TSC method in this epidemic disease, which involves 16 state variables with 3 control inputs, proves more complex compared to previous works with 4 state variables and 1 control input in [21], as well as 7 state variables with 3 control inputs in [35]. Additionally, the ZVL epidemic disease involves the dynamics of vector-borne and reservoir subpopulations along with their corresponding measures.
- This study introduces an integrated approach that combines the TSC method with DA, aiming to enhance the performance of control mechanisms for disease eradication. This integrated approach is designed to strengthen both techniques, contributing to a more effective control strategy.
- The significant improvement in convergence rates achieved by the proposed TSC method, compared to the conventional SC method, highlights improved convergence properties. This suggests the potential for more efficient control of ZVL through the integrated approach.

II. THE DYNAMIC OF ZOONOTIC VISCERAL LEISHMANIASIS

As feedback control and optimal control approaches have been successfully applied in various epidemic contexts [13-35], the ZVL epidemic model proposed in [13], among other ZVL mathematical models developed in previous works [9, 12-14], attracted significant research attention in this study. One reason is that the proposed control policies are implantable in practical situations such as vaccination control for dogs and human hospitalization [13, 14]. Instead of applying the annihilation or culling policy on the animal reservoir, the vaccination control policy was employed to avoid ethical concerns [13]. This study used the model developed in [13] to employ the TSC method to define multiple control policies for the ZVL epidemic system.

According to [13], three populations, vectors (sandflies), animal reservoirs (dogs), and humans, are contained in the leishmaniasis transmission model. The subpopulations corresponding to each population are defined as follows. First, the dog population consists of four subpopulations of dogs which are Susceptible (S), exposed (E), infectious (I), and recovered (R) subpopulations, denoted as S_d, E_d, I_d and R_d, respectively. Second, three subpopulations of the sandflies are susceptible, exposed, and infected subpopulations, defined as S_f, E_f and I_f, respectively. Third, the human population is divided into five subpopulations including susceptible, exposed, infected, Hospitalized, and recovered subpopulations, represented by S_h, E_h, I_h, H_h and $R_h$respectively. The dynamic transmission of ZVL, representing the interaction among the dog, sandfly, and human populations, is presented in (1), (2), and (3) as follows [13]:

Dog population:

$$\left.\begin{aligned}
\dot{S}_d &= \lambda_d + \rho N_d - \frac{b_{fd}\beta_{fd}I_f S_d(1-u_1(t))}{N_d} - \mu_d S_d \\
\dot{E}_d &= \frac{b_{fd}\beta_{fd}I_f S_d(1-u_1(t))}{N_d} - \tau_d E_d - \mu_d E_d \\
\dot{I}_d &= \tau_d E_d - r_d I_d - d_d I_d - \mu_d I_d \\
\dot{R}_d &= r_d I_d - \mu_d R_d
\end{aligned}\right\} \quad (1)$$

Sandfly population:

$$\left.\begin{aligned}
\dot{S}_f &= \lambda_f N_f(1-u_2(t)) - \frac{b_{fd}\beta_{df}I_d S_f}{N_d} \\
&\quad -(m_f + \mu_1 + \mu_2 N_f + r_0 u_2(t))S_f \\
\dot{E}_f &= \frac{b_{fd}\beta_{df}I_d S_f}{N_d} - \tau_f E_f - m_f E_f \\
&\quad -(\mu_1 + \mu_2 N_f)E_f - r_0 u_2(t)E_f \\
\dot{I}_f &= \tau_f E_f - d_f I_f - m_f I_f - (\mu_1 + \mu_2 N_f)I_f \\
&\quad -r_0 u_2(t) I_f
\end{aligned}\right\} \quad (2)$$

Human population:

$$\left.\begin{aligned}
\dot{S}_h &= \lambda_h + \gamma_h N_h - \frac{b_{fh}\beta_{fh} I_f S_h (1-u_3(t))}{N_h} - \mu_h S_h \\
\dot{E}_h &= \frac{b_{fh}\beta_{fh} I_f S_h (1-u_3(t))}{N_h} - \tau_h E_h - \mu_h E_h \\
\dot{I}_h &= \tau_h E_h - \delta_h I_h - d_I I_h - r_I I_h - \mu_h I_h \\
\dot{H}_h &= \delta_h I_h - d_H H_h - r_H H_h - \mu_h H_h \\
\dot{R}_h &= r_H H_h + r_I I_h - \mu_h R_h
\end{aligned}\right\} \quad (3)$$

where $N_d = S_d + E_d + I_d + R_d$, $N_f = S_f + E_f + I_f$, and $N_h = S_h + E_h + I_h + H_h + R_h$. The parameters of the ZVL epidemic system in (1), (2), and (3) are defined as follows. The birth rates corresponding to the dog, sandfly, and human populations are denoted by λ_d, λ_f and λ_h, respectively. The life span of the dog, sandfly, and human populations are represented by μ_d, μ_f, and μ_h, consecutively. The parameters of the average biting rate per infected sandfly to dog and human are defined by b_{fd} and b_{fh} , successively. The parameters, β_{fd} , β_{df} and β_{fh} represent the transmission probabilities from infected sandfly to dog, from infected dog to susceptible sandfly, and from infected sandfly to susceptible human, respectively. The death rates caused by the visceral leishmaniasis of dog, sandfly, and human populations are denoted by d_f , d_I and d_H , consecutively. The incubation periods of dog, sandfly, and human populations are represented by τ_d, τ_f and τ_h, successively. The recovery rate of infected dogs is r_d . The recovery rate of recovered humans from both natural and hospitalized recovery are r_I and r_H, respectively. The parameter δ is referred to as the rate of hospitalization for humans. Three control policies were applied in this model based on [13]. $u_1(t)$ represents the effectiveness of vaccination as a preventive measure, $u_2(t)$ indicates the effectiveness of the insecticide used at breeding sites for the sand fly population, and $u_3(t)$ reflects the effectiveness of personal protection measures designed to reduce sandfly-human interactions in the human population. All control policies are constrained as $0 \le u_i(t) \le 1, \forall i = \{1,2,3\}$.

The mathematical model in (1), (2), and (3) can be arranged in the affine nonlinear state space form containing state vector, $x = [S_d\ E_d\ I_d\ R_d\ S_f\ E_f\ I_f\ S_h\ E_h\ I_h\ H_h\ R_h]^T$, and control vector, $u = [u_1 \quad u_2 \quad u_3]^T$, as:

$$\dot{x} = f(x) + g(x)u \quad (4)$$

where:

$$f(x) = \begin{bmatrix} f_1(x) \\ f_2(x) \\ f_3(x) \\ f_4(x) \\ f_5(x) \\ f_6(x) \\ f_7(x) \\ f_8(x) \\ f_9(x) \\ f_{10}(x) \\ f_{11}(x) \\ f_{12}(x) \end{bmatrix} =$$

$$\begin{bmatrix}
\lambda_d + \rho N_d - \frac{b_{fd}\beta_{fd} x_7 x_1}{N_d} - \mu_d x_1 \\
\frac{b_{fd}\beta_{fd} x_7 x_1}{N_d} - \tau_d x_2 - \mu_d x_2 \\
\tau_d x_2 - r_d x_3 - d_d x_3 - \mu_d x_3 \\
r_d x_3 - \mu_d x_4 \\
\lambda_f N_f - \frac{b_{fd}\beta_{df} x_3 x_5}{N_d} - (m_f + \mu_1 + \mu_2 N_f) x_5 \\
\frac{b_{fd}\beta_{df} x_3 x_5}{N_d} - \tau_f x_6 - m_f x_6 - (\mu_1 + \mu_2 N_f) x_6 \\
\tau_f x_6 - d_f x_7 - m_f x_7 - (\mu_1 + \mu_2 N_f) x_7 \\
\lambda_h + \gamma_h N_h - \frac{b_{fh}\beta_{fh} x_7 x_8}{N_h} - \mu_h x_8 \\
\frac{b_{fh}\beta_{fh} x_7 x_8}{N_h} - \tau_h x_9 - \mu_h x_9 \\
\tau_h x_9 - \delta_h x_{10} - d_I x_{10} - r_I x_{10} - \mu_h x_{10} \\
\delta_h x_{10} - d_H x_{11} - r_H x_{11} - \mu_h x_{11} \\
r_H x_{11} + r_I x_{10} - \mu_h x_{12}
\end{bmatrix}$$

and:

$$g(x) = \begin{bmatrix}
g_1(x) & 0 & 0 \\
g_2(x) & 0 & 0 \\
0 & 0 & 0 \\
0 & 0 & 0 \\
0 & g_5(x) & 0 \\
0 & g_6(x) & 0 \\
0 & g_7(x) & 0 \\
0 & 0 & g_8(x) \\
0 & 0 & g_9(x) \\
0 & 0 & 0 \\
0 & 0 & 0 \\
0 & 0 & 0
\end{bmatrix}$$

with $g_1(x) = \frac{b_{fd}\beta_{fd} x_7 x_1}{N_d}$, $g_2(x) = -\frac{b_{fd}\beta_{fd} x_7 x_1}{N_d}$, $g_5(x) = -(r_0 x_5 + \lambda_f N_f)$, $g_6(x) = -r_0 x_6$, $g_7(x) = -r_0 x_7$, $g_8(x) = \frac{b_{fh}\beta_{fh} x_7 x_8}{N_h}$, and $g_9(x) = -\frac{b_{fh}\beta_{fh} x_7 x_8}{N_h}$.

For further details of the ZVL epidemic system, readers can consult [13].

III. THE CONTROL POLICY FOR THE ZOONOTIC VISCERAL LEISHMANIASIS EPIDEMIC SYSTEM

A. Terminal Synergetic Controller (TSC) Design

Considering the formulation of the optimal control presented in [13], the control objective to determine the multiple control policies using the feedback control approach is defined such that the exposed dog subpopulation x_2, the total sandfly population N_f, and the exposed human subpopulation x_9 approach to zero as time increases. Consequently, the corresponding reference signals are set as $x_{2r} = 0$, $N_{fr} = 0$, and $x_{9r} = 0$.

This study employed the TSC method proposed in [50]. In this approach, the Proportional and Integral (PI) type macro variable was defined so that the terminal attraction is satisfied. Importantly, it is beneficial to use this macro variable, since the singularity in the control input can be prevented by the integral expression [53, 54].

Based on [39, 42, 43, 45, 47, 50, 51], the process of synthesizing the TSC method to regulate the subpopulation can be presented as follows.

First, to improve the convergence properties of the control system, the macro variables were selected as follows [50]:

$$\left.\begin{aligned}\psi_2 &= k_{p2}e_2(t) + k_{i2}\int_o^t {e_2}^{q_2/p_2}(\tau)d\tau\\ \psi_f &= k_{pf}e_f(t) + k_{if}\int_o^t {e_f}^{q_f/p_f}(\tau)d\tau\\ \psi_9 &= k_{p9}e_9(t) + k_{i9}\int_o^t {e_9}^{q_9/p_9}(\tau)d\tau\end{aligned}\right\} \quad (5)$$

where e_2, e_f, and e_9 are tracking errors denoted as: $e_2 = x_2 - x_{2r}$, $e_f = N_f - N_{fr}$, and $e_9 = x_9 - x_{9r}$. The coefficients, k_{p2}, k_{i2}, k_{pf}, k_{if}, k_{p9} and k_{i9} are positive real numbers. The exponent terms, p_2, q_2, p_f, q_f, p_9 and q_9 are positive real odd numbers with $1 < \frac{p_i}{q_i} < 2$, $\forall i = \{2, f, 9\}$. These are the controller parameters. Their selection affects the convergence rate of each tracking error to zero.

Second, the dynamic evolutions of the macro variables in (5) are expressed as (6) [42, 43, 45, 47, 50, 51]:

$$\left.\begin{aligned}T_2\dot{\psi}_2 + \psi_2 &= 0\\ T_f\dot{\psi}_f + \psi_f &= 0\\ T_9\dot{\psi}_9 + \psi_9 &= 0\end{aligned}\right\} \quad (6)$$

where T_2, T_f, and T_9 are positive numbers. The convergence rate of each macro variable to the corresponding dynamic evolution depends on these parameters.

After substituting macro variables in (5) into (6), the dynamic evolutions become (7):

$$\left.\begin{aligned}T_2(k_{p2}\dot{e}_2 + k_{i2}{e_2}^{q_2/p_2}) + \psi_2 &= 0\\ T_f(k_{pf}\dot{e}_f + k_{if}{e_f}^{q_f/p_f}) + \psi_f &= 0\\ T_9(k_{p9}\dot{e}_9 + k_{i9}{e_9}^{q_9/p_9}) + \psi_9 &= 0\end{aligned}\right\} \quad (7)$$

Based on the ZVL epidemic system in (4) and dynamic evolution in (7), the multiple control policies can be obtained as (8):

$$\left.\begin{aligned}u_1 &= g_2(x)^{-1}\{{k_{p2}}^{-1}[-{T_2}^{-1}\psi_2 - k_{i2}{e_2}^{q_2/p_2}] - f_2(x)\}\\ u_2 &= g_f(x)^{-1}\{{k_{pf}}^{-1}[-{T_f}^{-1}\psi_f - k_{if}{e_f}^{q_f/p_f}] - f_f(x)\}\\ u_3 &= g_9(x)^{-1}\{{k_{p9}}^{-1}[-{T_9}^{-1}\psi_9 - k_{i9}{e_9}^{q_9/p_9}] - f_9(x)\}\end{aligned}\right\} \quad (8)$$

where $f_f(x) \triangleq f_5(x) + f_6(x) + f_7(x)$, and $g_f(x) \triangleq g_5(x) + g_6(x) + g_7(x)$.

B. Control System Stability

The proof of stability of the control system is referred to in [50] and is divided into two parts. The first part is to prove the stability of the dynamic evolution. Then, the stability of each tracking error corresponding to the control objective is proved in the second part. To investigate the stability of the set of dynamic evolutions, the Lyapunov function is defined as (9):

$$V_1 = 0.5{\psi_2}^2 + 0.5{\psi_f}^2 + 0.5{\psi_9}^2 \quad (9)$$

The derivative of V can be found in (10):

$$\dot{V}_1 = \psi_2\dot{\psi}_2 + \psi_f\dot{\psi}_f + \psi_9\dot{\psi}_9 \quad (10)$$

Considering the dynamic evolution in (6), the derivative of the Lyapunov function can be expressed as (11):

$$\begin{aligned}\dot{V}_1 &= \psi_2(-{T_2}^{-1}\psi_2) + \psi_f(-{T_f}^{-1}\psi_f) + \psi_9(-T^{-1}\psi_9)\\ &= -{T_2}^{-1}{\psi_2}^2 - {T_f}^{-1}{\psi_f}^2 - T^{-1}{\psi_9}^2 \le 0\end{aligned} \quad (11)$$

The derivative of the Lyapunov function in (11) shows that the macro variables converge to zero by the control input in (8).

Next, the proof of the stability of the dynamic errors, $e_2(t)$, $e_f(t)$ and $e_9(t)$ when $\psi_2 = 0$, $\psi_f = 0$ and $\psi_9 = 0$ can be performed as follows. The Lyapunov of the error dynamic is defined as (12):

$$V_2 = 0.5{e_2}^2 + 0.5{e_f}^2 + 0.5{e_9}^2 \quad (12)$$

and the derivative of (12) is founded in (13):

$$\dot{V}_2 = e_2\dot{e}_2 + e_f\dot{e}_f + e_9\dot{e}_9 \quad (13)$$

According to (5), with $\psi_2 = 0$, $\psi_f = 0$ and $\psi_9 = 0$, the derivatives of the dynamic errors can be determined as (14):

$$\left.\begin{aligned}\dot{e}_2(t) &= -\frac{k_{i2}}{k_{p2}}{e_2}^{q_2/p_2}\\ \dot{e}_f(t) &= -\frac{k_{if}}{k_{pf}}{e_f}^{q_f/p_f}\\ \dot{e}_9(t) &= -\frac{k_{i9}}{k_{p9}}{e_9}^{q_9/p_9}\end{aligned}\right\} \quad (14)$$

Then, (13) can be written as (15):

$$\begin{aligned}\dot{V}_2 &= e_2\left(-\frac{k_{i2}}{k_{p2}}{e_2}^{\frac{q_2}{p_2}}\right) + e_f\left(-\frac{k_{if}}{k_{pf}}{e_f}^{\frac{q_f}{p_f}}\right) + e_9\left(-\frac{k_{i9}}{k_{p9}}{e_9}^{\frac{q_9}{p_9}}\right) =\\ &-\frac{k_{i2}}{k_{p2}}{e_2}^{\left(\frac{q_2}{p_2}\right)+1} - \frac{k_{if}}{k_{pf}}{e_f}^{\left(\frac{q_f}{p_f}\right)+1} - \frac{k_{i9}}{k_{p9}}{e_9}^{\left(\frac{q_9}{p_9}\right)+1} = -\frac{k_{i2}}{k_{p2}}{e_2}^{\frac{q_2+p_2}{p_2}} -\\ &\frac{k_{if}}{k_{pf}}{e_f}^{(q_f+p_f)/p_f} - \frac{k_{i9}}{k_{p9}}{e_9}^{(q_9+p_9)/p_9}\end{aligned} \quad (15)$$

The numerators of the exponent terms are even numbers and can be written as $(q_2 + p_2) = 2s_2$, $(q_f + p_f) = 2s_f$ and $(q_9 + p_9) = 2s_9$, where s_2, s_f, and s_9 are positive integers. Then, the derivative of V_2 can be found in (16):

$$\begin{aligned}\dot{V}_2 &= -\frac{k_{i2}}{k_{p2}}{e_2}^{2s_2/p_2} - \frac{k_{if}}{k_{pf}}{e_f}^{2s_f/p_f} - \frac{k_{i9}}{k_{p9}}{e_9}^{2s_9/p_9}\\ &= -\frac{k_{i2}}{k_{p2}}({e_2}^{\frac{s_2}{p_2}})^2 - \frac{k_{if}}{k_{pf}}({e_f}^{\frac{s_f}{p_f}})^2\\ &-\frac{k_{i9}}{k_{p9}}({e_9}^{s_9/p_9})^2 \le 0\end{aligned} \quad (16)$$

Equation (16) implies that all tracking errors converge to zero when the macro variables are zero. Thus, according to (11) and (16), the designed control policies in (8) can manipulate the state variables corresponding to the control objective to the desired levels.

Remark 1: For the boundedness of the rest states, from (16), it is known that N_f is finite, hence x_5, x_6, and x_7 are all

bounded since $N_f = x_5 + x_6 + x_7$ and the nonnegativity of the states x_1 to x_{12} [13]. By considering (67) and (69) of [13], if some suitable parameters and initial conditions are chosen, then the boundedness of N_d is guaranteed, thus the states x_1 to x_4 are bounded by $N_d = x_1 + x_2 + x_3 + x_4$. A similar argument can be stated for the boundedness of states x_8 to x_{12} whenever some suitable parameters and initial conditions are chosen.

Remark 2: The parameters k_{i2}, k_{p2}, k_{if}, k_{pf}, k_{i9}, k_{p9}, T_2, T_f, and T_9 are all responding to the tuning rate of convergence of each variable that it corresponds with. To illustrate, from (16), the parameters k_{i2}, k_{p2}, k_{if}, k_{pf}, k_{i9}, and k_{p9} are related to the rate of convergence of the Lyapunov function $V_2(e_2, e_f, e_9)$. The larger of $\frac{k_{i2}}{k_{p2}}$, $\frac{k_{if}}{k_{pf}}$, and $\frac{k_{i9}}{k_{p9}}$, the faster the Lyapunov function $V_2(e_2, e_f, e_9)$ converges to zero. For T_2, T_f, and T_9, considering (6) $\forall i = \{2, f, 9\}$

$$T_i \dot{\psi}_i(t) + \psi_i(t) = 0$$

$$\psi_i(t) = \psi_i(0) e^{-\frac{1}{T_i}}$$

Hence, the parameters T_2, T_f, and T_9 correspond to the rate of convergence of $\psi_i(t)$ for $i = 2, f, 9$, respectively.

C. Controller Parameters Tuning Using Dragonfly Algorithm

In this study, the DA is applied to optimize the performance of the ZVL control system by setting the optimal values of control parameters. The original MATLAB code for the DA was modified [58], and Figure 1 illustrates the modified DA. The goal is to find the best combination of parameters to minimize a specific objective function. The tuning objective function (myObj.m) is defined to allow the DA to be called with a set of varying tuning parameters for simulation in each iteration. The objective function initiates the simulation, subsequently returning the objective as the summation of u^2, i.e. ${u_1}^2 + {u_2}^2 + {u_3}^2$. The main.m function of the original DA has been edited to configure *fobj*=@*myObj*, and *dim*=9, as the number of tuning parameters. The nine control parameters were chosen as follows: k_{i2}, k_{if},k_{i9}, k_{p2}, k_{pf},k_{p9}, T_2, T_f, and T_9.

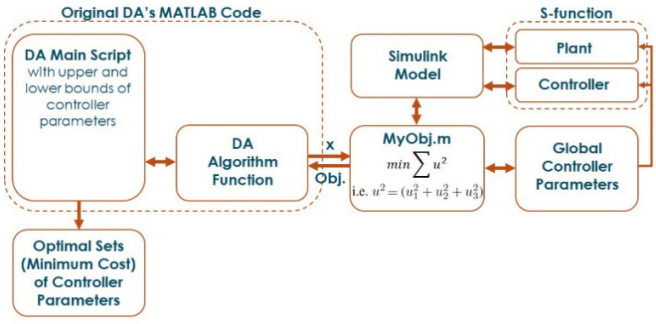

Fig. 1. The diagram of the DA for TSC control parameters tuning.

IV. SIMULATION

Initially, the simulation example of the ZVL epidemic system, controlled by the multiple policies outlined in (8), is introduced. Subsequently, the second subsection presents the simulation results and corresponding discussions.

A. Simulation Example

The mathematical model of the ZVL with the numerical parameters was from [13] and the literature therein. Then, the designed TSC method in (8) was employed to demonstrate the feasibility and performance of the proposed method.

The numerical values of system parameters were from the [13, 59-61] as follows: $\lambda_d = 0.02$, $\lambda_f = 0.05$, $\lambda_h = 0.05$, ${\mu_d}^{-1} = 700$, ${\mu_h}^{-1} = 12{,}000$, $b_{fd} = 0.1$, $b_{fh} = 0.1$, $\beta_{fd} = 0.5$, $\beta_{df} = 0.7$, $\beta_{fh} = 0.5$, $d_d = 0.01$, $d_f = 0$, $d_I = 0.0067$, $d_H = 3 \times 10^{-4}$, $m_f = 1 \times 10^{-4}$, ${\tau_d}^{-1} = 10$, ${\tau_f}^{-1} = 6$, ${\tau_h}^{-1} = 60$, $\delta_h = 0.8$, $r_d = 0.01$, $r_I = 0.12$, $r_H = 0.95$, $\rho = 1 \times 10^{-3}$, $\mu_1 = 0.02$, $\mu_2 = 5 \times 10^{-6}$, $r_0 = 0.2$, and $\gamma_h = 2.85 \times 10^{-3}$.

The control inputs are constrained as $0 \le u_1 \le 0.6$, $0 \le u_2 \le 0.5$, and $0 \le u_3 \le 0.6$. The upper bound of each control strategy was set based on [13], which assumes that the effectiveness of each control strategy may not be fully achieved.

Nine controller parameters are derived from DA. To prevent singularity (when some parameter equals 0) in the control calculations, the lower bounds are established as follows: i) $k_{i2} = k_{if} = k_{i9} = 0.01$, ii) $k_{p2} = k_{pf} = k_{p9} = 0.5$, and iii) $T_2 = T_f = T_9 = 0.0003$.

The upper bounds are established as follows: i) $k_{i2} = k_{if} = k_{i9} = 0.2$, ii) $k_{p2} = k_{pf} = k_{p9} = 2.0$ and iii) $T_2 = T_f = T_9 = 20.0$.

After 18 iterations, DA yields the optimal set of TSC control parameters as follows: $k_{i2} = 0.01$, $k_{if} = 0.01$, $k_{i9} = 0.2$, $k_{p2} = 2.0$, $k_{pf} = 2.0$, $k_{p9} = 1.1134$, $T_2 = 20$, $T_f = 20$, and $T_9 = 0.04717$. The cost function decreased from 2840 to a minimum of 2660, as illustrated in the convergence curve plot in Figure 2.

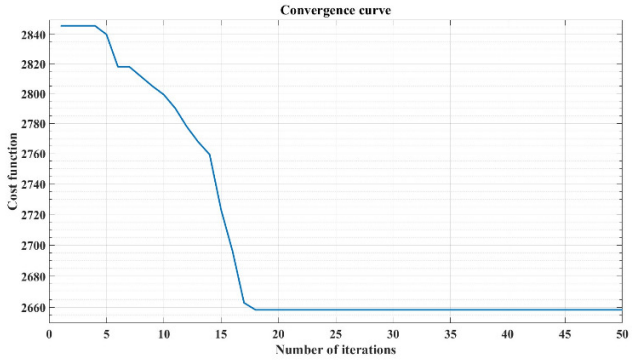

Fig. 2. The convergence curve of DA for TSC control parameters tuning.

- To present the improvement of the convergence rate, the TSC method was performed and compared with the conventional SC method. The conventional SC method was synthesized in the same procedure as that of the TSC

method. However, the macro variables were defined as $\psi_2 = k_{p2}e_2(t)$, $\psi_f = k_{pf}e_{Nf}(t)$ and $\psi_9 = k_{p9}e_9(t)$. The simulation time is from $t = 0$ to $t = 300$ days. In the simulation, the Runge-Kutta method was used to solve the state variable of the control system.

B. *Simulation Results and Discussion*

The example of the control system was simulated. Figure 3 shows a plot of state variables according to the control objective including the exposed dog subpopulation x_2, the total sandfly population N_f, and the exposed human subpopulation x_9. Figure 4 shows the time responses of all infected subpopulations, including infected dogs x_3, sandflies x_7, and humans x_{10}. Figure 5 shows the multiple control policies consisting of the vaccination control for the dog population u_1, the annihilation or insecticide of the sandfly u_2, and the prevention control for the human population u_3

The plot of time responses in Figure 3 shows that the TSC method could regulate the state variables according to the control objective. The exposed dog subpopulation, total sandfly population, and exposed human subpopulation converge to zero as time increases. In addition, the TSC method provided better convergence rates compared to the results of the conventional SC method.

In addition, the time responses of the infected dog subpopulation x_3, infected sandfly subpopulation x_7, and human subpopulation x_{10} under the TSC method and the conventional SC method were compared in Figure 4. Under the multiple control policies given by the TSC method, all infected subpopulations approached zero as time increased. Moreover, the convergence rates of the infected subpopulations, when controlled by the TSC method, surpassed those controlled by the conventional SC method.

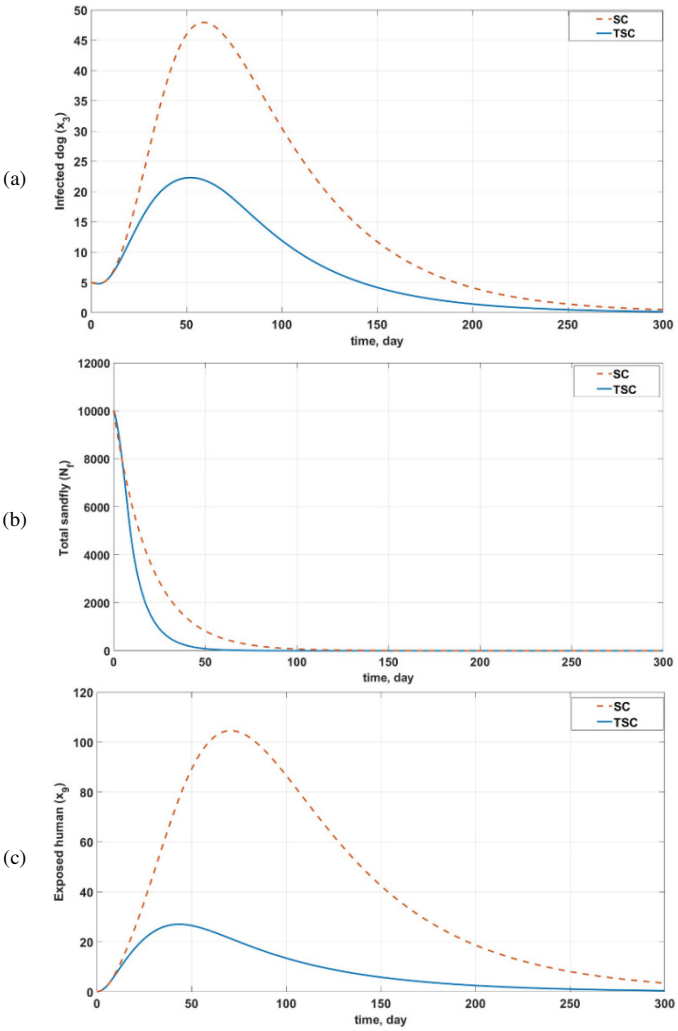

Fig. 3. Comparison of the convergence rates between the TSC and SC methods for exposed subpopulations: (a) Exposed dog subpopulations, (b) Total sandfly populations, (c) Exposed human subpopulations.

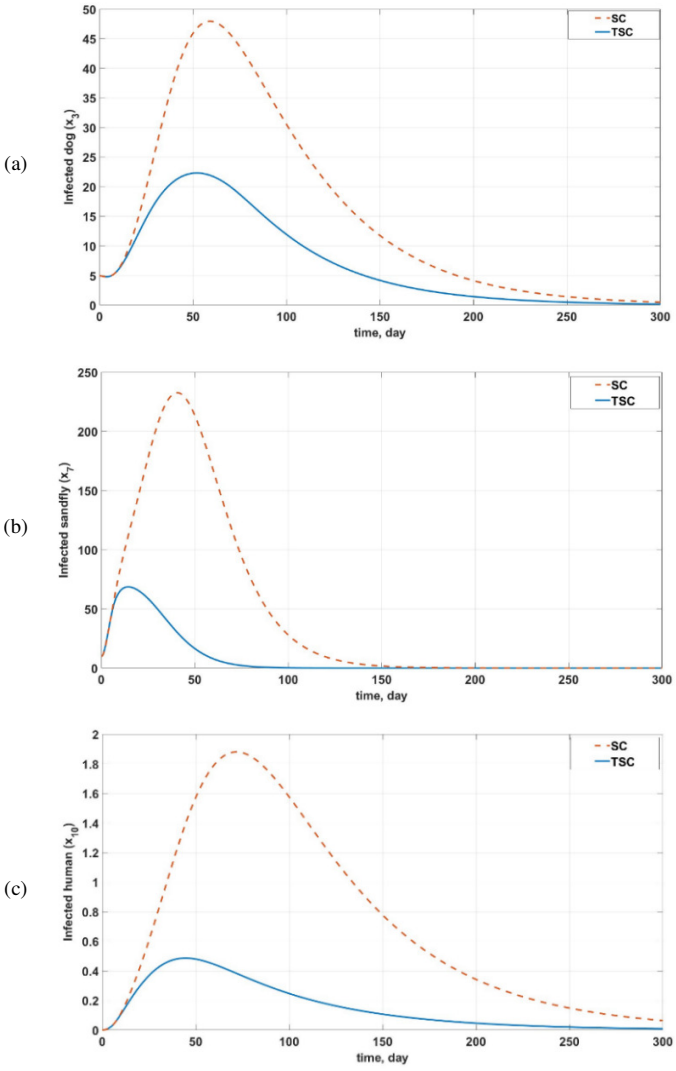

Fig. 4. Comparison of the convergence rates between the TSC and SC methods for infected subpopulations: (a) Infected dog subpopulations, (b) Infected sandfly subpopulations, (c) Infected human subpopulations.

In Figure 5(a), it is observed that the vaccination control for the dog population, as per the conventional SC method, remained at the maximum level from the initial time to the final time. In contrast, the TSC method initiated at the maximum level and experienced a reduction from 30 to 70 days, reaching the minimum level of 0.22 at 60 days. In Figure 5(b), the insecticide control for the sandfly population in both approaches reveals an initiation from initial positive values, stabilizing at different levels. Notably, for insecticide control, the TSC method requires a faster increase toward a higher maximum level than the conventional SC method. The personal protections employed by both TSC and SC controllers reached the same maximum levels, as shown in Figure 5(c).

(a)

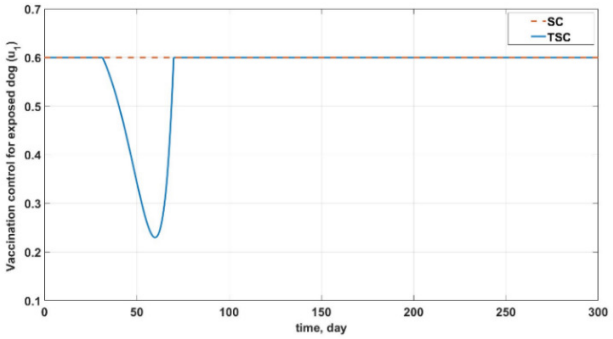

(b)

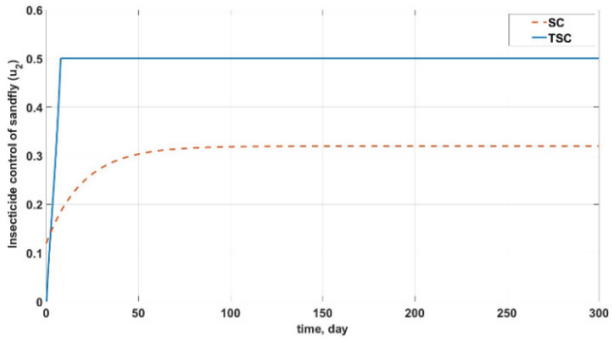

(c)

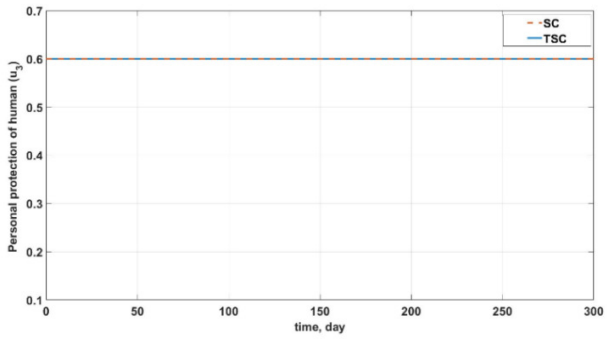

Fig. 5. Comparison of the control policies between the TSC and SC methods: (a) Vaccination control for exposed dog subpopulations, (b) Insecticide control of sandfly subpopulations, (c) Personal protection of human subpopulations.

Although the TSC method required a higher control effort than the conventional SC method, the time responses of all target subpopulations with optimal controller parameters converged more rapidly to the desired levels. This improved efficiency is crucial for the eradication of the ZVL epidemic. As expected, the multiple control policies adhered to the chattering-free characteristic, an essential aspect for practical policy application. Additionally, including terminal attraction with integral expression in the synthesized control law successfully avoided singularity in the control signal. Although the TSC method requires greater control efforts, it facilitates faster stabilization of key epidemiological variables at the desired levels, making it more effective in situations where rapid disease containment is essential. However, the method's sustainability depends on balancing its increased control demands with long-term feasibility, particularly in resource-constrained areas. Compared to traditional approaches, such as the SC method, the TSC approach is more responsive, offering significant advantages in regions with high transmission rates of vector-borne diseases, including ZVL. From a practical perspective, integrating vaccine protection, sandfly control, and personal protection into a comprehensive strategy can significantly improve epidemiological outcomes, especially in developing regions where the disease burden is high.

The proposed TSC controller could serve as a guideline for implementing healthcare resource planning in real-world situations, including strategies for vaccination, insecticide use, and other interventions. The proposed control law can be viewed as a lower-bounded controller for policymakers to manage the infected population and achieve fixed-time stability. Furthermore, this study suggests an optimal solution by tuning the parameters using DA to enhance the controller's implementability.

V. CONCLUSION

This research focused on the application of the TSC method to determine multiple control policies for the eradication of ZVL. These policies encompass vaccination for the dog population, insecticide treatment of sandflies, and personal prevention measures for humans. The integration of the DA facilitated the optimization of the control parameters, enhancing the performance of the TSC method. Singularity prevention in control input signals was achieved through terminal attraction with the integral expression. Based on numerical simulations, the TSC method could manipulate the state variables so that the control objective was satisfied. The corresponding all-infected subpopulations converged to zero. The selection of macro variables with terminal attraction could enhance the convergence rate of the control leishmaniasis epidemic system compared to the conventional SC method. Furthermore, having chattering-free control inputs is beneficial and practical when implementing epidemic prevention and control policies. This research serves as a feasible strategy for developing robust control mechanisms to eradicate vector-borne diseases.

REFERENCES

[1] "Control of the leishmaniases WHO TRS no. 949," World Health Organization, Mar. 2010. [Online]. Available: https://www.who.int/publications/i/item/WHO-TRS-949.

[2] R. Lainson, R. D. Ward, J. J. Shaw, and P. C. C. Garnham, "Leishmania in phlebotomid sandflies: VI. Importance of hindgut development in distinguishing between parasites of the Leishmania mexicana and L.

braziliensis complexes," *Proceedings of the Royal Society of London. Series B. Biological Sciences*, vol. 199, no. 1135, pp. 309–320, Jan. 1997, https://doi.org/10.1098/rspb.1977.0141.

[3] P. Kaye and P. Scott, "Leishmaniasis: complexity at the host–pathogen interface," *Nature Reviews Microbiology*, vol. 9, no. 8, pp. 604–615, Aug. 2011, https://doi.org/10.1038/nrmicro2608.

[4] E. Torres-Guerrero, M. R. Quintanilla-Cedillo, J. Ruiz-Esmenjaud, and R. Arenas, "Leishmaniasis: a review," *F1000Research*, vol. 6, May 2017, Art. no. 750, https://doi.org/10.12688/f1000research.11120.1.

[5] N. Singh, J. Mishra, R. Singh, and S. Singh, "Animal Reservoirs of Visceral Leishmaniasis in India," *Journal of Parasitology*, vol. 99, no. 1, pp. 64–67, Feb. 2013, https://doi.org/10.1645/GE-3085.1.

[6] J. Alvar *et al.*, "Leishmaniasis Worldwide and Global Estimates of Its Incidence," *PLOS ONE*, vol. 7, no. 5, 2012, Art. no. e35671, https://doi.org/10.1371/journal.pone.0035671.

[7] World Health Organization, "Leishmaniasis." https://www.who.int/news-room/fact-sheets/detail/leishmaniasis.

[8] K. J. Evans and L. Kedzierski, "Development of Vaccines against Visceral Leishmaniasis," *Journal of Tropical Medicine*, vol. 2012, no. 1, 2012, Art. no. 892817, https://doi.org/10.1155/2012/892817.

[9] H. J. Shimozako, J. Wu, and E. Massad, "Mathematical modelling for Zoonotic Visceral Leishmaniasis dynamics: A new analysis considering updated parameters and notified human Brazilian data," *Infectious Disease Modelling*, vol. 2, no. 2, pp. 143–160, May 2017, https://doi.org/10.1016/j.idm.2017.03.002.

[10] I. Elmojtaba and R. Altayeb, "An Optimal Control Model for the Dynamics of Visceral Leishmaniasis," *International Journal of Mathematical and Computational Sciences*, vol. 2, Dec. 2015.

[11] S. Biswas, "Mathematical modeling of Visceral Leishmaniasis and control strategies," *Chaos, Solitons & Fractals*, vol. 104, pp. 546–556, Nov. 2017, https://doi.org/10.1016/j.chaos.2017.09.005.

[12] I. M. ELmojtaba, J. Y. T. Mugisha, and M. H. A. Hashim, "Mathematical analysis of the dynamics of visceral leishmaniasis in the Sudan," *Applied Mathematics and Computation*, vol. 217, no. 6, pp. 2567–2578, Nov. 2010, https://doi.org/10.1016/j.amc.2010.07.069.

[13] S. Zhao, Y. Kuang, C.-H. Wu, D. Ben-Arieh, M. Ramalho-Ortigao, and K. Bi, "Zoonotic visceral leishmaniasis transmission: modeling, backward bifurcation, and optimal control," *Journal of Mathematical Biology*, vol. 73, no. 6, pp. 1525–1560, Dec. 2016, https://doi.org/10.1007/s00285-016-0999-z.

[14] L. M. Ribas, V. L. Zaher, H. J. Shimozako, and E. Massad, "Estimating the Optimal Control of Zoonotic Visceral Leishmaniasis by the Use of a Mathematical Model," *The Scientific World Journal*, vol. 2013, no. 1, 2013, Art. no. 810380, https://doi.org/10.1155/2013/810380.

[15] H. Puebla, P. K. Roy, A. Velasco-Perez, and M. M. Gonzalez-Brambila, "Biological pest control using a model-based robust feedback," *IET Systems Biology*, vol. 12, no. 6, pp. 233–240, 2018, https://doi.org/10.1049/iet-syb.2018.5010.

[16] Y. Xiao, X. Xu, and S. Tang, "Sliding Mode Control of Outbreaks of Emerging Infectious Diseases," *Bulletin of Mathematical Biology*, vol. 74, no. 10, pp. 2403–2422, Oct. 2012, https://doi.org/10.1007/s11538-012-9758-5.

[17] M. De la Sen, R. P. Agarwal, R. Nistal, S. Alonso-Quesada, and A. Ibeas, "A switched multicontroller for an SEIADR epidemic model with monitored equilibrium points and supervised transients and vaccination costs," *Advances in Difference Equations*, vol. 2018, no. 1, Oct. 2018, Art. no. 390, https://doi.org/10.1186/s13662-018-1839-9.

[18] M. D. la Sen, A. Ibeas, and S. Alonso-Quesada, "Feedback linearization-based vaccination control strategies for true-mass action type SEIR epidemic models," *Nonlinear Analysis: Modelling and Control*, vol. 16, no. 3, pp. 283–314, Jul. 2011, https://doi.org/10.15388/NA.16.3.14094.

[19] M. De la Sen, A. Ibeas, and S. Alonso-Quesada, "On vaccination controls for the SEIR epidemic model," *Communications in Nonlinear Science and Numerical Simulation*, vol. 17, no. 6, pp. 2637–2658, Jun. 2012, https://doi.org/10.1016/j.cnsns.2011.10.012.

[20] A. Ibeas, M. De La Sen, and S. Alonso-Quesada, "Sliding mode robust control of SEIR epidemic models," in *2013 21st Iranian Conference on Electrical Engineering (ICEE)*, Mashhad, Iran, May 2013, pp. 1–6, https://doi.org/10.1109/IranianCEE.2013.6599820.

[21] A. Boonyaprapasorn, S. Natsupakpong, P. S. Ngiamsunthorn, and K. Thung-od, "An application of finite time synergetic control for vaccination in epidemic systems," in *2017 IEEE Conference on Systems, Process and Control (ICSPC)*, Malacca, Spain, Dec. 2017, pp. 30–35, https://doi.org/10.1109/SPC.2017.8313017.

[22] A. Boonyaprapasorn, S. Kuntanapreeda, P. S. Ngaimsunthorn, T. Sethaput, and T. Kumsaen, "HBV Epidemic Control Using Time-Varying Sliding Mode Control Method," *Proceedings of International Conference on Artificial Life and Robotics*, vol. 27, pp. 205–212, Jan. 2022, https://doi.org/10.5954/ICAROB.2022.GS3-3.

[23] A. Boonyaprapasorn, S. Kuntanapreeda, P. S. Ngaimsunthorn, T. Kumsaen, and T. Sethaput, "Fractional Order Sliding Mode Controller for HBV Epidemic System," *Mathematical Modelling of Engineering Problems*, vol. 09, no. 06, pp. 1622–1630, Dec. 2022, https://doi.org/10.18280/mmep.090623.

[24] A. Boonyaprapasorn, P. S. Ngiamsunthorn, and T. Sethaput, "Synergetic control for HIV infection system of CD4+T cells," in *2016 16th International Conference on Control, Automation and Systems (ICCAS)*, Gyeongju, South Korea, Oct. 2016, pp. 484–488, https://doi.org/10.1109/ICCAS.2016.7832364.

[25] S. Alonso-Quesada, M. De la Sen, and R. Nistal, "An SIRS Epidemic Model Supervised by a Control System for Vaccination and Treatment Actions Which Involve First-Order Dynamics and Vaccination of Newborns," *Mathematics*, vol. 10, no. 1, Jan. 2022, Art. no. 36, https://doi.org/10.3390/math10010036.

[26] G. Albi, L. Pareschi, and M. Zanella, "Control with uncertain data of socially structured compartmental epidemic models," *Journal of Mathematical Biology*, vol. 82, no. 7, May 2021, Art. no. 63, https://doi.org/10.1007/s00285-021-01617-y.

[27] S. Boubaker, "A Predictive Vaccination Strategy Based on a Swarm Intelligence Technique for the Case of Saudi Arabia: A Control Engineering Approach," *Engineering, Technology & Applied Science Research*, vol. 13, no. 4, pp. 11091–11095, Aug. 2023, https://doi.org/10.48084/etasr.5987.

[28] M. Fliess, C. Join, and A. d'Onofrio, "Feedback control of social distancing for COVID-19 via elementary formulae," *IFAC-PapersOnLine*, vol. 55, no. 20, pp. 439–444, Jan. 2022, https://doi.org/10.1016/j.ifacol.2022.09.134.

[29] T. Berger, "Feedback control of the COVID-19 pandemic with guaranteed non-exceeding ICU capacity," *Systems & Control Letters*, vol. 160, Feb. 2022, Art. no. 105111, https://doi.org/10.1016/j.sysconle.2021.105111.

[30] M. D. la Sen, A. Ibeas, and A. Garrido, "On a new SEIRDEoIo epidemic model eventually initiated from outside with delayed re-susceptibility and vaccination and treatment feedback controls," *Physica Scripta*, vol. 96, no. 9, Mar. 2021, Art. no. 095002, https://doi.org/10.1088/1402-4896/ac018c.

[31] M. Sharifi and H. Moradi, "Nonlinear robust adaptive sliding mode control of influenza epidemic in the presence of uncertainty," *Journal of Process Control*, vol. 56, pp. 48–57, Aug. 2017, https://doi.org/10.1016/j.jprocont.2017.05.010.

[32] M. Alutto, G. Como, and F. Fagnani, "On SIR epidemic models with feedback-controlled interactions and network effects," in *2021 60th IEEE Conference on Decision and Control (CDC)*, Austin, TX, USA, Dec. 2021, pp. 5562–5567, https://doi.org/10.1109/CDC45484.2021.9683007.

[33] M. Bisiacco and G. Pillonetto, "Sliding-Mode Theory Under Feedback Constraints and the Problem of Epidemic Control," *SIAM Journal on Applied Mathematics*, vol. 83, no. 6, pp. 2189–2211, Dec. 2023, https://doi.org/10.1137/22M1535309.

[34] L. A. Alarcón-Ramos, R. Bernal Jaquez, and A. Schaum, "Output-Feedback Control of Virus Spreading in Complex Networks With Quarantine," *Frontiers in Applied Mathematics and Statistics*, vol. 4, Aug. 2018, https://doi.org/10.3389/fams.2018.00034.

[35] A. Boonyaprapasorn *et al.*, "Control of Ebola Epidemic System Based on Terminal Synergetic Controller Design," in *2019 IEEE International Conference on Automatic Control and Intelligent Systems (I2CACIS)*,

Selangor, Malaysia, Jun. 2019, pp. 204–209, https://doi.org/10.1109/I2CACIS.2019.8825074.

[36] A. Boonyaprapasorn, S. Simatrang, S. Kuntanapreeda, P. S. Ngiamsunthorn, T. Kumsaen, and T. Sethaput, "Terminal Synergetic Control for Plate Heat Exchanger," *Journal of Advanced Research in Fluid Mechanics and Thermal Sciences*, vol. 117, no. 1, pp. 189–202, May 2024, https://doi.org/10.37934/arfmts.117.1.189202.

[37] J. Y. Suen and S. Navlakha, "A feedback control principle common to several biological and engineered systems," *Journal of The Royal Society Interface*, vol. 19, no. 188, Mar. 2022, Art. no. 20210711, https://doi.org/10.1098/rsif.2021.0711.

[38] S. Alonso-Quesada, M. De la Sen, R. Agarwal, and A. Ibeas, "An observer-based vaccination control law for an SEIR epidemic model based on feedback linearization techniques for nonlinear systems," *Advances in Difference Equations*, vol. 2012, no. 1, Sep. 2012, Art. no. 161, https://doi.org/10.1186/1687-1847-2012-161.

[39] A. A. Kolesnikov, "Introduction of synergetic control," in *2014 American Control Conference*, Portland, OR, USA, Jun. 2014, pp. 3013–3016, https://doi.org/10.1109/ACC.2014.6859397.

[40] A. A. Kolesninkov, *Synergetics control theory*. Moscow, Russia: Energoatomizdat, 1994.

[41] A. A. Kolesnikov, Modern applied control theory: Synergetic approach in control theory. Moscow, Russia: Integracia-TSURE, 2000.

[42] E. Santi, A. Monti, D. Li, K. Proddutur, and R. A. Dougal, "Synergetic control for DC-DC boost converter: implementation options," *IEEE Transactions on Industry Applications*, vol. 39, no. 6, pp. 1803–1813, Aug. 2003, https://doi.org/10.1109/TIA.2003.818967.

[43] E. Santi, A. Monti, D. Li, K. Proddutur, and R. A. Dougal, "Synergetic control for power electronics applications: a comparison with the sliding mode approach," *Journal of Circuits, Systems and Computers*, vol. 13, no. 04, pp. 737–760, Aug. 2004, https://doi.org/10.1142/S0218126604001520.

[44] I. Kondratiev, Synergetic control: Converter based autonomous DC power distribution systems. Lap Lambert Academic Publishing, 2009.

[45] A. A. Kolesnikov and A. S. Mushenko, "Applied Theory of Nonlinear System Design: Method Comparison," in *2019 III International Conference on Control in Technical Systems (CTS)*, St. Petersburg, Russia, Oct. 2019, pp. 50–53, https://doi.org/10.1109/CTS48763.2019.8973304.

[46] I. Kondratiev, E. Santi, and R. Dougal, "Robust nonlinear synergetic control for m-parallel-connected DC-DC boost converters," in *2008 IEEE Power Electronics Specialists Conference*, Rhodes, Greece, Jun. 2008, pp. 2222–2228, https://doi.org/10.1109/PESC.2008.4592272.

[47] G. E. Veselov, A. A. Sklyarov, and S. A. Sklyarov, "Synergetic approach to quadrotor helicopter control with attractor-repeller strategy of nondeterministic obstacles avoidance," in *2014 6th International Congress on Ultra Modern Telecommunications and Control Systems and Workshops (ICUMT)*, St. Petersburg, Russia, Oct. 2014, pp. 228–235, https://doi.org/10.1109/ICUMT.2014.7002107.

[48] S. Zhai, Q. Chen, and X. Tang, "Finite-Time Synergetic Control of Mechanical System Based on Model-Free Friction Compensation," in *Proceedings of the 2015 Chinese Intelligent Automation Conference*, 2015, pp. 275–284, https://doi.org/10.1007/978-3-662-46463-2_29.

[49] C. H. Liu and M. Y. Hsiao, "A finite time synergetic control scheme for robot manipulators," *Computers & Mathematics with Applications*, vol. 64, no. 5, pp. 1163–1169, Sep. 2012, https://doi.org/10.1016/j.camwa.2012.03.058.

[50] C. H. Liu and M. Y. Hsiao, "Synchronization on unified chaotic systems via PI-type terminal synergetic control," in *2013 CACS International Automatic Control Conference (CACS)*, Nantou, Taiwan, Dec. 2013, pp. 24–29, https://doi.org/10.1109/CACS.2013.6734101.

[51] A. Hachana and M. N. Harmas, "Terminal Synergetic Control for Blood Glucose Regulation in Diabetes Patients," *Journal of Dynamic Systems, Measurement, and Control*, vol. 140, no. 100801, May 2018, https://doi.org/10.1115/1.4039716.

[52] A. Boonyaprapasorn, S. Simatrang, S. Kuntanapreeda, and T. Sethaput, "Application of the Terminal Synergetic Control for Biological Control of Sugarcane Borer," *IEEE Access*, vol. 12, pp. 49562–49577, 2024, https://doi.org/10.1109/ACCESS.2024.3384608.

[53] Z. Zuo, "Non-singular fixed-time terminal sliding mode control of non-linear systems," *IET Control Theory & Applications*, vol. 9, no. 4, pp. 545–552, 2015, https://doi.org/10.1049/iet-cta.2014.0202.

[54] J. B. Wang, C. X. Liu, Y. Wang, and G. C. Zheng, "Fixed time integral sliding mode controller and its application to the suppression of chaotic oscillation in power system*," *Chinese Physics B*, vol. 27, no. 7, Apr. 2018, Art. no. 070503, https://doi.org/10.1088/1674-1056/27/7/070503.

[55] S. Mirjalili, "Dragonfly algorithm: a new meta-heuristic optimization technique for solving single-objective, discrete, and multi-objective problems," *Neural Computing and Applications*, vol. 27, no. 4, pp. 1053–1073, May 2016, https://doi.org/10.1007/s00521-015-1920-1.

[56] A. Boonyaprapasorn, S. Kuntanapreeda, P. S. Ngiamsunthorn, T. Kumsaen, and T. Sethaput, "Time-varying sliding mode controller for heat exchanger with dragonfly algorithm," *International Journal of Electrical and Computer Engineering (IJECE)*, vol. 13, no. 4, Aug. 2023, Art. no. 3958, https://doi.org/10.11591/ijece.v13i4.pp3958-3968.

[57] A. I. Hammouri, M. Mafarja, M. A. Al-Betar, M. A. Awadallah, and I. Abu-Doush, "An improved Dragonfly Algorithm for feature selection," *Knowledge-Based Systems*, vol. 203, Sep. 2020, Art. no. 106131, https://doi.org/10.1016/j.knosys.2020.106131.

[58] S. Mirjalili, "Dragonfly Algorithm Toolbox," 2022. https://www.mathworks.com/matlabcentral/fileexchange/51031-dragonfly-algorithm-toolbox.

[59] K. W. Blayneh, A. B. Gumel, S. Lenhart, and T. Clayton, "Backward Bifurcation and Optimal Control in Transmission Dynamics of West Nile Virus," *Bulletin of Mathematical Biology*, vol. 72, no. 4, pp. 1006–1028, May 2010, https://doi.org/10.1007/s11538-009-9480-0.

[60] N. Hartemink *et al.*, "Integrated Mapping of Establishment Risk for Emerging Vector-Borne Infections: A Case Study of Canine Leishmaniasis in Southwest France," *PLOS ONE*, vol. 6, no. 8, 2011, Art. no. e20817, https://doi.org/10.1371/journal.pone.0020817.

[61] A. Stauch *et al.*, "Visceral Leishmaniasis in the Indian Subcontinent: Modelling Epidemiology and Control," *PLOS Neglected Tropical Diseases*, vol. 5, no. 11, 2011, Art. no. e1405, https://doi.org/10.1371/journal.pntd.0001405.